

Infrared Emittance of Water Clouds

PETR CHÝLEK* AND PETER DAMIANO

Atmospheric Science Program, Department of Physics and Oceanography, Dalhousie University, Halifax, Nova Scotia, Canada

ERIC P. SHETTLE

Optical Sciences Division, Naval Research Laboratory, Washington, D.C.

(Manuscript received 20 June 1991, in final form 19 November 1991)

ABSTRACT

A simple approximation has been developed for the infrared emittance of clouds composed of water spheres based on the absorption approximation for the emittance and on the polynomial approximation to the Mie absorption efficiency. The expression for the IR emittance is obtained in a simple analytical form as a function of the liquid water content and two size distribution parameters, namely, the effective radius and effective variance. The approximation is suitable for numerical weather prediction, climate modeling, and radiative transfer calculations. The accuracy, when compared to the exact Mie calculation and integration over the size distribution, is within a few percent, while the required computer time is reduced by several orders of magnitude. In the limit of small droplet sizes, the derived IR emittance reduces to a term proportional to the liquid water content.

1. Introduction

Cloud emittance in the infrared region of the spectrum and especially within the atmospheric window between 8 and 13 μm is an important factor in any study concerning the climate, climatic change, and cloud-radiation feedback. Although the radiative transfer formalism together with the Mie scattering and absorption provide means to calculate cloud emittance at any wavelength for given size distribution of the spherical particles, such calculations are time consuming and presently are unsuitable for use in climate or numerical weather prediction models. Consequently, a simple parameterization in the form of the cloud's bulk properties (like liquid water content) has been sought (e.g., Paltridge 1974; Platt 1975, 1976; Cox 1976; Stephens 1978; Chýlek and Ramaswamy 1982) and used in climate modeling (e.g., Ramanathan 1983; Stephens 1984).

With the realization that the cloud-radiation feedback (e.g., Schneider 1972; Paltridge 1980; Ohring and Clapp 1980; Charlock 1982; Sommerville and Remer 1984; Stephens et al. 1990) may modify the predicted

change of climate, a need arises for a more accurate treatment of cloud infrared emittance. A simple expression is needed that, however, would still allow the study of changes of emittance connected with the evolution of the cloud's microstructure.

The microstructure and optical properties of water and ice clouds have been a subject of recent intensive research (Platt 1981; Platt and Stephens 1980; Platt et al. 1987; Platt and Harshvardhan 1988). Most of the ice cloud particles are obviously nonspherical. In the region of the solar radiation, geometrical optics can be used to account for hexagonal columns and plates (Liou 1980; Takano and Liou 1989). However, at infrared wavelengths the ice crystal size is not necessarily large compared to the wavelength, so geometric optics is not a suitable approximation. Because of the lack of a general approximation for the scattering and absorption of radiation by nonspherical particles, ice clouds are often treated as if composed of effective spheres (e.g., Stephens et al. 1990; Ackerman et al. 1990; Smith et al. 1990; Spinhirne and Hart 1990) with a suitably defined effective radius. Since ice crystals can grow in size up to several hundreds of micrometers (e.g., Heymsfield 1986; Heymsfield et al. 1990), an emittance formulation that can be extended to the region of large radii spheres is needed.

We derive a simple expression for the infrared emittance, which is computationally fast for use in numerical models and shows an explicit dependence on the liquid water content as well as on two other parameters, specifying the size distribution that may be chosen in

* Also affiliated with: Department of Atmospheric Science and Atmospheric Sciences Research Center, State University of New York at Albany, New York.

Corresponding author address: Dr. Petr Chýlek, Atmospheric Science Program, Department of Physics and Oceanography, Dalhousie University, Halifax, B3H 3J5, Canada.

the form of an effective radius and effective variance. We demonstrate that the proposed approximation is accurate to within a few percent when compared to exact Mie calculations for all droplet sizes with radii up to 100 μm . Extensions to even larger particles can be easily achieved. In the limit of small particles our expression for the infrared emittance reduces to the currently used bulk approximation in the form of liquid water content.

2. Infrared emittance and currently used approximations

At an arbitrary wavelength in the IR spectral region the emittance ϵ of a homogeneous cloud layer can be written in the zero-scattering approximation (e.g., Hunt 1973; Paltridge and Platt 1976; Stephens et al. 1990) as

$$\epsilon = 1 - e^{-k_{\text{abs}}z}, \quad (1)$$

where z is the cloud's geometrical thickness. In the case of spherical cloud particles the absorption coefficient k_{abs} is given by

$$k_{\text{abs}} = \pi \int r^2 Q_{\text{abs}}(r) n(r) dr, \quad (2)$$

where r is the radius of a spherical particle, $n(r)$ is the size distribution, and $Q_{\text{abs}}(r)$ is the absorption efficiency (or the absorption cross section per unit projected area of a particle).

The absorption coefficient k_{abs} , and thus the emittance ϵ , can be obtained for any given size distribution $n(r)$ at the chosen wavelength from Mie scattering calculations (e.g., van de Hulst 1957) for the absorption efficiency Q_{abs} at each particle radius r and performing numerical integration over the cloud particle size distribution. However, such a procedure is cumbersome and makes large demands on computer time. It is therefore not the best suited for cloud emittance calculations in climate studies or for radiation calculations in mesoscale cloud models. A simple expression relating the emittance ϵ or the absorption coefficient k_{abs} to the cloud's bulk property (water content W) and to a few parameters defining the size distribution is desired.

a. Small particle case

A simple approximation eliminating the emittance dependence on the cloud's microstructure has been proposed and used extensively (e.g., Platt 1975, 1976; Chýlek and Ramaswamy 1982; Stephens 1984). The approximation is based on the observation (Fig. 1) that for wavelengths $\lambda > 3 \mu\text{m}$ the Mie absorption efficiency Q_{abs} can be reasonably well approximated by a linear function of the radius r for $r < r_{\text{max}}$. The value of r_{max} varies between 5 and 13 μm , depending on the wavelength within the spectral region of interest (Chýlek

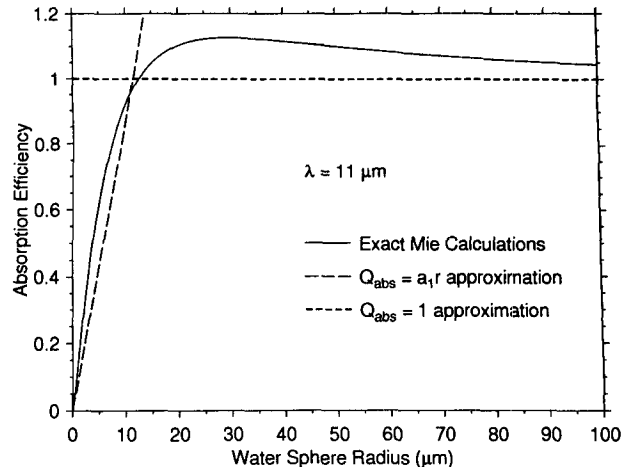


FIG. 1. The Mie absorption efficiency Q_{abs} has often been approximated by a linear function of radii for the case of small droplet radii and by a constant $Q_{\text{abs}} = 1$ for the case of large droplets.

1978; Pinnick et al. 1979, 1980; Chýlek and Ramaswamy 1982).

Using this approximation for the absorption efficiency,

$$Q_{\text{abs}} = a_1 r, \quad (3)$$

the absorption coefficient k_{abs} can be expressed as a function of the water content,

$$W = \frac{4\pi\rho}{3} \int r^3 n(r) dr, \quad (4)$$

in the form

$$k_{\text{abs}} = \frac{3a_1}{4\rho} W, \quad (5)$$

where ρ is the density of water or ice, as appropriate.

The advantage of expression (5) for the absorption coefficient k_{abs} is its simplicity. The obvious disadvantage is the fact that we are limited to the small sizes of droplets for which the approximation is expected to be valid.

b. Large particle case

At least some water clouds and many cirrus clouds have particles large enough to violate the requirement on which the relation (5) is based. This is especially the case when cirrus cloud particles are modeled by equivalent spheres (Stephens et al. 1990; Spinhirne and Hart 1990; Smith et al. 1990; Ackerman et al. 1990). The effective radius of these spheres (often between 20 and 100 μm) is usually found to be far above the limits of applicability of the simple approximation for the absorption efficiency and the absorption coefficients represented by Eqs. (3) and (5). For these large particles a different approximation to Q_{abs} , as calculated

by the Mie theory, seems to be more appropriate. As Q_{abs} approaches a large-particle asymptotic limit close to 1, we can assume that for large spherical particles

$$Q_{\text{abs}} = a_0, \tag{6}$$

where a_0 is a constant close to 1 (Fig. 1). Substitution of this approximation for the absorption efficiency (6) into the absorption coefficient integral (2), together with the relation for the water content (4), leads to the following expression (e.g., Stephens et al. 1990; Platt and Harshvardhan 1988; Chýlek 1978) for the absorption coefficient:

$$k_{\text{abs}} = \frac{3a_0}{4\rho r_{\text{eff}}} W, \tag{7}$$

where the effective radius r_{eff} of a size distribution $n(r)$ is defined (e.g., Hansen and Travis 1974) as the area-weighted mean radius,

$$r_{\text{eff}} = \frac{\int r^3 n(r) dr}{\int r^2 n(r) dr}. \tag{8}$$

The dependence of the cloud emittance on the cloud's microstructure is expressed in the form of the effective radius r_{eff} of the size distribution. The advantage of this form of approximation is that it considers more accurately the contribution of large particles, which is particularly important for the case of ice clouds. This size dependence of the emittance in the form of $1/r_{\text{eff}}$ appears to be confirmed by observations in the case of cirrus clouds (Platt and Harshvardhan 1988; Smith et al. 1990). However, as shown by Fig. 1, the absorption efficiency of small particles is considerably overestimated by this approximation, and even the efficiency of large particles is not well represented by a constant value of $Q_{\text{abs}} = 1$.

3. Polynomial approximation for Q_{abs}

We propose a simple approximation for the infrared emittance of clouds composed of spherical particles or represented by effective spheres. Any useful approximation should retain a simple form so that it can be used in parameterization of radiative processes in numerical weather prediction and climate models. For computational convenience it is also desirable that the approximation retains an analytic form when integrated over representative size distributions. At the same time, a more physically rigorous approach than that presented in section 2 is desirable.

The absorption efficiency Q_{abs} , as calculated using the Mie scattering formalism for a moderately absorbing medium, does not show significant oscillations as a function of droplet radius (Fig. 1). It can be expected that such a curve can be accurately approximated by an N th degree polynomial with a moderate value of N

for droplet radii smaller than some chosen maximum value r_{max} . For the case of water clouds we chose $r_{\text{max}} = 100 \mu\text{m}$, and we write

$$Q_{\text{abs}} = \sum_{n=0}^N a_n r^n, \tag{9}$$

where the a_n are the expansion coefficients that can be determined at required wavelengths by least-squares polynomial fit to the Mie calculation and tabulated for future use. Substitution of this expansion into expression (2) gives a simple expression for the absorption coefficient of a size distribution in the form

$$k_{\text{abs}} = \pi \sum_{n=0}^N a_n m_{n+2}, \tag{10}$$

where the n th moment m_n of the size distribution $n(r)$ is defined as

$$m_n = \int r^n n(r) dr \tag{11}$$

with n being zero or a positive integer. Equation (10) is the basic result of the proposed approximation. In the rest of this section we simply recast this result into a more convenient form.

For most analytic size distributions, $n(r)$, the required moments can be usually expressed as simple functions of the size distribution parameters. An arbitrary moment m_n can be also expressed in terms of the third moment m_3 by a relation of the form

$$m_n = C_n m_3, \tag{12}$$

where C_n is a constant for a given n and a specific size distribution.

Alternatively, one may explicitly separate out the factors of the effective radius r_{eff} from the C_n , which will permit rewriting the expression for the absorption coefficient [Eq. (10)] as a power series in the effective radius,

$$m_n = D_n m_3 (r_{\text{eff}})^{n-3}, \tag{13}$$

where $D_n = C_n / r_{\text{eff}}^{n-3}$.

Using relation (12) or (13), the expression (10) for the absorption coefficient k_{abs} of a size distribution can be written as

$$k_{\text{abs}}(\lambda) = \frac{3W}{4\rho} \sum_{n=0}^N a_n(\lambda) C_{n+2}, \tag{14}$$

or

$$k_{\text{abs}}(\lambda) = \frac{3W}{4\rho} \sum_{n=0}^N a_n(\lambda) D_{n+2} r_{\text{eff}}^{n-1}. \tag{15}$$

In the expressions (14) and (15) the relation between the third moment of the size distribution and the liquid water content W ,

$$m_3 = \frac{3W}{4\pi\rho}, \quad (16)$$

has been used. Also, the dependence on wavelength has been explicitly shown to emphasize that the C_n and the D_n are functions only of the size distribution, independent of wavelength. Equation (15) suggests that the expansion of the Q_{abs} curve in the power series of r leads to the power series expansion of the absorption coefficient k_{abs} in an effective radius r_{eff} where the lowest power present is r_{eff}^{-1} .

The first three terms of the power series expansion (15) are independent of the form of the size distribution used. They can be written as functions of the liquid water content W , the effective radius r_{eff} , and the effective variance v_{eff} . For example, the second moment is

$$m_2 = \frac{3W}{4\pi\rho r_{\text{eff}}}. \quad (17)$$

If we further define an effective variance v_{eff} as (Hansen and Travis 1974)

$$v_{\text{eff}} = \frac{\int (r - r_{\text{eff}})^2 r^2 n(r) dr}{r_{\text{eff}}^2 \int r^2 n(r) dr} = \frac{m_4 m_2}{m_3^2} - 1, \quad (18)$$

we can write the fourth moment as

$$m_4 = \frac{3W}{4\pi\rho} r_{\text{eff}} (1 + v_{\text{eff}}). \quad (19)$$

Substituting the expressions for the second, third, and fourth moments of a size distribution, (16), (17), and (19), into the expansion of the absorption coefficient (10) leads to

$$k_{\text{abs}} = \frac{3W}{4\rho} \left[\frac{a_0}{r_{\text{eff}}} + a_1 + a_2 r_{\text{eff}} (1 + v_{\text{eff}}) + \sum_{n=3}^N a_n \frac{m_{n+2}}{m_3} \right], \quad (20)$$

where the first three terms are written outside the sum in their explicit form. We wish to emphasize that the forms of expressions, (10), (14), (15), and (20), are independent of the form of the size distribution used.

Comparing Eq. (20) with (14), it follows that the first three C_k are given by

$$C_2 = 1/r_{\text{eff}}, \quad C_3 = 1, \quad \text{and} \quad C_4 = r_{\text{eff}} (1 + v_{\text{eff}}), \quad (21)$$

and the corresponding D_k are given by

$$D_2 = D_3 = 1 \quad \text{and} \quad D_4 = 1 + v_{\text{eff}}. \quad (22)$$

These values for the C_k and the D_k depend only on the effective radius [Eq. (8)] and the effective variance [Eq. (18)] and are independent of the details of the size distribution. To calculate the higher-order ($k \geq 5$) coefficients C_k and D_k or the moments m_n , we need to consider the specific form of the size distribution used.

a. Gamma size distribution

It has been shown (Deirmendjian 1969; Hansen and Travis 1974; Chýlek and Ramaswamy 1982; Stephens et al. 1990; Stephens and Tsay 1990) that many of the size distributions of aerosols, fogs, and cloud particles can be well represented by a gamma-type distribution of the form

$$n(r) = Ar^\alpha e^{-\beta r}, \quad (23)$$

where A , α , and β are constants specifying the distribution. These parameters can be related to the total number of particles per unit volume N_0 , to the effective radius r_{eff} , and to the effective variance v_{eff} as follows:

$$N_0 = A \frac{\Gamma(\alpha + 1)}{\beta^{\alpha+1}}, \quad (24)$$

$$r_{\text{eff}} = \frac{\alpha + 3}{\beta}, \quad (25)$$

and

$$v_{\text{eff}} = 1/(\alpha + 3), \quad (26)$$

where Γ is the usual gamma function (e.g., Abramowitz and Stegun 1964).

For the n th moment of the size distribution (23) we obtain

$$m_n = A \frac{\Gamma(\alpha + n + 1)}{\beta^{\alpha+n+1}}. \quad (27)$$

Using the recurrence relation for the gamma function $\Gamma(z) = (z - 1)\Gamma(z - 1)$, the following expression for the ratio of the moments, m_{n+2}/m_3 , can be derived:

$$\frac{m_{n+2}}{m_3} = \frac{(\alpha + n + 2)!}{(\alpha + 3)! \beta^{n-1}}, \quad (28)$$

where the definition of the factorial function is extended to include noninteger values (Abramowitz and Stegun 1964).

Substituting the ratio of the moments [Eq. (28)] into the expansion of the absorption coefficient in terms of the moments [Eq. (10)] leads to the following expression for the absorption coefficient:

$$k_{\text{abs}} = \frac{3W}{4\rho} \sum_{n=0}^N a_n \frac{(\alpha + n + 2)!}{(\alpha + 3)! \beta^{n-1}}. \quad (29)$$

If we write the first three terms explicitly in terms of W , r_{eff} , and v_{eff} , we can rewrite (29) as

$$k_{\text{abs}} = \frac{3W}{4\rho} \left[\frac{a_0}{r_{\text{eff}}} + a_1 + a_2 r_{\text{eff}} (1 + v_{\text{eff}}) + \sum_{n=3}^N a_n \frac{(\alpha + n + 2)!}{(\alpha + 3)! \beta^{n-1}} \right]. \quad (30)$$

Other useful forms of the absorption coefficient k_{abs} can be obtained from the general expressions (14) and

(15) using the form of C_k and D_k coefficients appropriate for the gamma size distribution

$$C_k = \frac{(\alpha + k)!}{(\alpha + 3)!} \beta^{3-k} = \frac{(\alpha + k)}{\beta} C_{k-1} \quad (31)$$

$$D_k = \frac{(\alpha + k)!}{(\alpha + 3)!(\alpha + 3)^{k-3}} = \frac{(\alpha + k)}{(\alpha + 3)} D_{k-1} \\ = \frac{(\alpha + k)(\alpha + k - 1) \cdots (\alpha + 4)}{(\alpha + 3)^{k-3}} \quad (32)$$

Consequently, regardless of how many terms in the polynomial expansion (9) of the absorption efficiency are kept, the absorption coefficient k_{abs} and the emittance ϵ can be always written as a function of total water content W and two additional parameters characterizing the size distribution. These two parameters can be chosen in any suitable form, which either characterizes the mathematical form of the size distribution (like α and β) or, as physically more meaningful quantities, the effective radius r_{eff} and effective variance v_{eff} .

We should remember that the coefficients a_n , appearing in expressions for k_{abs} , are constants that are determined in advance and tabulated for any desired wavelength.

b. Lognormal size distribution

The lognormal size distribution is frequently utilized to represent aerosol size distributions (for example, see Clark and Whitby 1967 or d'Almeida et al. 1991). A discussion of the properties of lognormal distributions is given by Aitchison and Brown (1957) and Allen (1968).

In the case of the lognormal size distribution,

$$n(r) = \frac{N_0}{rs\sqrt{2\pi}} \exp\left[-\frac{(\ln r - \ln r_0)^2}{2s^2}\right], \quad (33)$$

we obtain for the effective radius and effective variance,

$$r_{\text{eff}} = r_0 \exp(5s^2/2) \quad (34)$$

TABLE 1. Moments m_k , effective radius r_{eff} , effective variance v_{eff} , and expansion coefficients for absorption, C_k and D_k , for different size distributions.

Parameter	Gamma distribution	Lognormal distribution	Modified gamma	Sum of lognormal distributions
$n(r)$	$Ar^\alpha \exp(-\beta r)$	$\frac{N_0}{rs\sqrt{2\pi}} \exp\left[-\frac{(\ln r - \ln r_0)^2}{2s^2}\right]$	$Ar^\alpha \exp(-\beta r^\gamma)$	$\sum_i \frac{N_i}{r_i s_i \sqrt{2\pi}} \exp\left[-\frac{(\ln r - \ln r_i)^2}{2s_i^2}\right]$
m_k	$A \frac{(\alpha + k)!}{\beta^{\alpha+k+1}}$	$N_0 r_0^k \exp\left(\frac{s^2 k^2}{2}\right)$	$\frac{A}{\gamma} \beta^{-(\alpha+k+1)/\gamma} \Gamma\left(\frac{\alpha + k + 1}{\gamma}\right)$	$\sum_i N_i r_i^k \exp\left(\frac{s_i^2 k^2}{2}\right)$
$\frac{m_k}{m_j}$	$\frac{(\alpha + k)!}{(\alpha + j)!} \cdot \beta^{j-k}$	$r_0^{(k-j)} \exp\left[\frac{(k^2 - j^2)s^2}{2}\right]$	$\beta^{(j-k)/\gamma} \frac{\Gamma\left(\frac{\alpha + k + 1}{\gamma}\right)}{\Gamma\left(\frac{\alpha + j + 1}{\gamma}\right)}$	$\frac{\sum_i N_i r_i^k \exp\left(\frac{s_i^2 k^2}{2}\right)}{\sum_i N_i r_i^j \exp\left(\frac{s_i^2 j^2}{2}\right)}$
r_{eff}	$\frac{(\alpha + 3)}{\beta}$	$r_0 \exp\left(\frac{5s^2}{2}\right)$	$\frac{\Gamma\left(\frac{\alpha + 4}{\gamma}\right)}{\beta^{1/\gamma} \Gamma\left(\frac{\alpha + 3}{\gamma}\right)}$	$\frac{\sum_i N_i r_i^3 \exp\left(\frac{9s_i^2}{2}\right)}{\sum_i N_i r_i^2 \exp(2s_i^2)}$
v_{eff}	$\frac{1}{(\alpha + 3)}$	$\exp(s^2) - 1$	$\frac{\Gamma\left(\frac{\alpha + 5}{\gamma}\right) \Gamma\left(\frac{\alpha + 3}{\gamma}\right)}{\left[\Gamma\left(\frac{\alpha + 4}{\gamma}\right)\right]^2} - 1$	$\frac{[\sum_i N_i r_i^2 \exp(8s_i^2)][\sum_i N_i r_i^2 \exp(4s_i^2)]}{\left[\sum_i N_i r_i^3 \exp\left(\frac{9s_i^2}{2}\right)\right]^2}$
C_k	$\frac{(\alpha + k)!}{(\alpha + 3)!} \cdot \beta^{3-k}$	$r_0^{(k-3)} \exp\left[\frac{(k^2 - 9)s^2}{2}\right]$	$\beta^{(3-k)/\gamma} \frac{\Gamma\left(\frac{\alpha + k + 1}{\gamma}\right)}{\Gamma\left(\frac{\alpha + 4}{\gamma}\right)}$	$\frac{\sum_i N_i r_i^k \exp\left(\frac{s_i^2 k^2}{2}\right)}{\sum_i N_i r_i^3 \exp\left(\frac{9s_i^2}{2}\right)}$
D_k	$\frac{(\alpha + k)!}{(\alpha + 3)!(\alpha + 3)^{k-3}}$	$\exp\left[\frac{(k-2)(k-3)s^2}{2}\right]$	$\frac{\left[\Gamma\left(\frac{\alpha + 3}{\gamma}\right)\right]^{k-3} \Gamma\left(\frac{\alpha + k + 1}{\gamma}\right)}{\Gamma\left(\frac{\alpha + 4}{\gamma}\right)}$	$\left[\frac{\sum_i N_i r_i^k \exp\left(\frac{s_i^2 k^2}{2}\right)}{\sum_i N_i r_i^3 \exp\left(\frac{9s_i^2}{2}\right)}\right] \cdot r_{\text{eff}}^{(3-k)}$

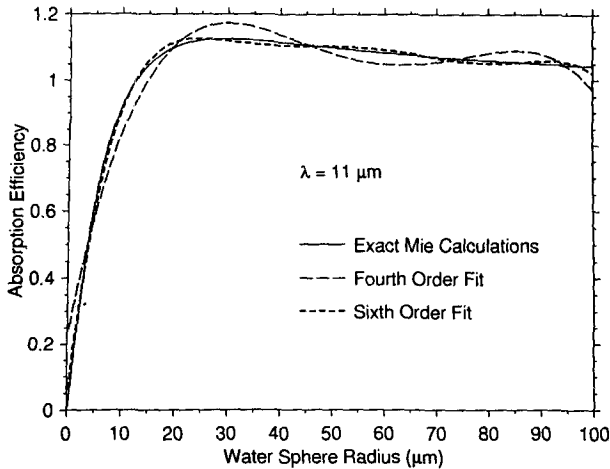


FIG. 2. At wavelength $\lambda = 11 \mu\text{m}$, the Mie absorption efficiency Q_{abs} can be very accurately approximated by the sixth-order polynomial for droplet radii up to $100 \mu\text{m}$. For the purposes of comparison, the fourth-order polynomial fit is also shown.

and

$$v_{\text{eff}} = \exp(s^2) - 1, \quad (35)$$

and for the moments of a lognormal distribution,

$$m_n = r_0^n N_0 \exp(s^2 n^2 / 2) \quad (36)$$

$$\frac{m_{n+2}}{m_3} = r_0^{n-1} \exp[s^2(n^2 + 4n - 5)/2]. \quad (37)$$

Finally, the absorption coefficient k_{abs} for the lognormal size distribution (33) is given by

$$k_{\text{abs}} = \frac{3W}{4\rho} \left[\frac{a_0}{r_{\text{eff}}} + a_1 + a_2 r_{\text{eff}} (1 + v_{\text{eff}}) + \sum_{n=3}^N a_n r_0^{n-1} \exp[s^2(n^2 + 4n - 5)/2] \right]. \quad (38)$$

Alternative forms of k_{abs} are obtained from (14) and (15) using

$$C_k = r_0^{k-3} \exp[s^2(k^2 - 9)/2] \quad (39)$$

and

$$D_k = \exp[s^2(k-2)(k-3)/2]. \quad (40)$$

c. Comparison of gamma and lognormal distributions

The coefficients D_k in the expansion of the absorption coefficient [Eq. (15)] as a power series in r_{eff} , for both the gamma and lognormal size distributions, can be written in terms of v_{eff} instead of the parameters α and s that define the size distributions. When this is done, with the use of the expression for v_{eff} [Eq. (26)]

for the gamma distribution, the expression for D_k [Eq. (32)] (for $k > 4$) becomes

$$D_k = (1 + v_{\text{eff}})(1 + 2v_{\text{eff}}) \cdots (1 + [k-3]v_{\text{eff}}). \quad (41)$$

Similarly, with the use of the expression for v_{eff} [Eq. (35)] for the lognormal distribution, the corresponding expression for D_k [Eq. (40)] becomes

$$D_k = (1 + v_{\text{eff}})^{(k-2)(k-3)/2}. \quad (42)$$

While these two expressions for D_k differ, as would be expected since the higher-order moments of the lognormal and gamma distributions differ, it can be shown that for $v_{\text{eff}} \ll 1$, both expressions (41) and (42) for the coefficients D_k can be approximated by

$$D_k = 1 + (k-2)(k-3)v_{\text{eff}}/2. \quad (43)$$

For typical cloud-droplet size distributions, the effective variances v_{eff} are generally small. For example, the cloud models developed by Carrier et al. (1967) have values of v_{eff} ranging from 0.11 to 0.25, and the cloud models from LOWTRAN 7, (Kneizys et al. 1988), used later in this paper, have values between 0.11 and 0.20.

d. Other size distributions

One can calculate the required moments or the C_k and D_k coefficients for any other desired form of the size distribution. We have done so for the cases of the modified gamma size distribution and for the multimodal size distribution composed of the superposition of the lognormal size distributions. The absorption coefficient k_{abs} can be calculated from expressions (10), (14), (15), or (20) using the C_k and D_k coefficients or the required moments presented in Table 1.

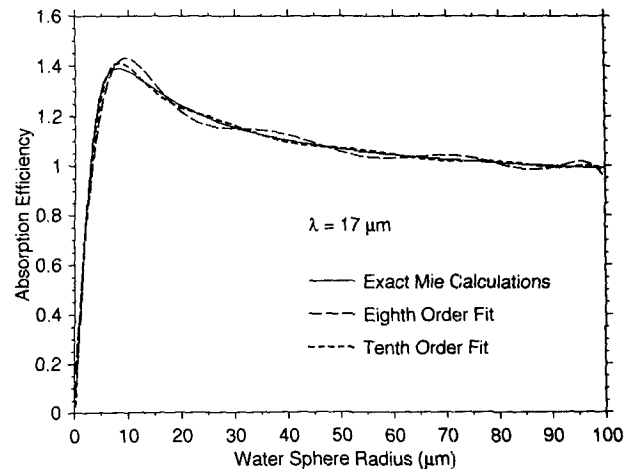


FIG. 3. At the wavelength $\lambda = 17 \mu\text{m}$, the tenth-order polynomial fit to the Mie absorption efficiency Q_{abs} is needed to achieve a sufficiently high degree of accuracy. For comparison the eighth-order polynomial fit is also shown.

TABLE 2a. Expansion coefficients, a_0 - a_5 , from the tenth-order polynomial fit to water drops with $r \leq 100 \mu\text{m}$.

Wavelength (μm)	a_0	a_1	a_2	a_3	a_4	a_5
3.0	6.9815E-1	3.4005E-1	-7.1149E-2	6.6926E-3	-3.5002E-4	1.1132E-5
3.5	-3.7180E-2	1.1072E-1	-8.6505E-3	4.7492E-4	-1.7057E-5	3.9811E-7
4.0	-9.6181E-3	3.4409E-2	4.4013E-4	-1.8546E-4	1.2994E-5	-4.7269E-7
4.5	-2.2915E-2	8.6545E-2	-1.2638E-3	-2.8739E-4	2.3789E-5	-9.0303E-7
5.0	-1.2561E-2	6.2228E-2	1.6466E-3	-4.6510E-4	3.0146E-5	-1.0410E-6
5.5	-5.3218E-3	4.6155E-2	2.2442E-3	-3.8078E-4	2.1056E-5	-6.4755E-7
6.0	-3.2700E-2	4.0000E-1	-5.2563E-2	3.7182E-3	-1.6065E-4	4.4652E-6
6.5	-4.1663E-2	1.6364E-1	-6.5303E-3	-2.0327E-4	2.8063E-5	-1.1529E-6
7.0	-2.5295E-2	1.1287E-1	-1.3311E-3	-2.7327E-4	2.6748E-5	-9.0158E-7
7.5	-2.4799E-2	1.0648E-1	-1.6453E-3	-2.4226E-4	1.6773E-5	-5.2631E-7
8.0	-2.5546E-2	1.0472E-1	-2.1762E-3	-1.4286E-4	1.0485E-5	-3.1804E-7
8.5	-2.5596E-2	1.0379E-1	-2.3913E-3	-1.0720E-4	8.7520E-6	-2.8032E-7
9.0	-2.4838E-2	1.0392E-1	-2.4856E-3	-1.0346E-4	9.2521E-6	-3.2065E-7
9.5	-2.3760E-2	1.0607E-1	-2.7200E-3	-9.9199E-5	9.8648E-6	-3.6047E-7
10.0	-2.2574E-2	1.1175E-1	-3.4213E-3	-6.3962E-5	9.0329E-6	-3.5283E-7
10.5	-2.3256E-2	1.3538E-1	-6.3175E-3	1.0099E-4	3.3355E-6	-2.2171E-7
11.0	-2.5803E-2	1.8682E-1	-1.3771E-2	6.0111E-4	-1.6791E-5	3.0421E-7
11.5	-2.4114E-2	2.5643E-1	-2.6010E-2	1.5583E-3	-6.0079E-5	1.5373E-6
12.0	-1.2646E-2	3.3011E-1	-4.0730E-2	2.8203E-3	-1.2106E-4	3.3597E-6
12.5	3.0035E-3	3.9705E-1	-5.4744E-2	4.0682E-3	-1.8309E-4	5.2531E-6
13.0	1.2844E-2	4.4196E-1	-6.4208E-2	4.9197E-3	-2.2580E-4	6.5657E-6
13.5	1.5736E-2	4.7796E-1	-7.1571E-2	5.5748E-3	-2.5846E-4	7.5661E-6
14.0	1.0228E-2	5.0398E-1	-7.6483E-2	5.9943E-3	-2.7884E-4	8.1788E-6
14.5	-1.0387E-3	5.2183E-1	-7.9414E-2	6.2230E-3	-2.8924E-4	8.4760E-6
15.0	-1.4490E-2	5.3560E-1	-8.1383E-2	6.3598E-3	-2.9485E-4	8.6217E-6
15.5	-2.8565E-2	5.4678E-1	-8.2779E-2	6.4429E-3	-2.9768E-4	8.6806E-6
16.0	-4.5099E-2	5.5482E-1	-8.3341E-2	6.4422E-3	-2.9602E-4	8.5948E-6
16.5	-6.1469E-2	5.6013E-1	-8.3308E-2	6.3862E-3	-2.9152E-4	8.4203E-6
17.0	-7.8866E-2	5.6057E-1	-8.2104E-2	6.2172E-3	-2.8110E-4	8.0587E-6
17.5	-9.5654E-2	5.5933E-1	-8.0536E-2	6.0139E-3	-2.6891E-4	7.6416E-6
18.0	-1.1096E-1	5.5380E-1	-7.8066E-2	5.7290E-3	-2.5262E-4	7.0986E-6
18.5	-1.2451E-1	5.4493E-1	-7.4923E-2	5.3845E-3	-2.3339E-4	6.4665E-6
19.0	-1.3602E-1	5.3259E-1	-7.1098E-2	4.9809E-3	-2.1129E-4	5.7485E-6
19.5	-1.4485E-1	5.1540E-1	-6.6326E-2	4.4962E-3	-1.8528E-4	4.9150E-6
20.0	-1.4756E-1	4.9338E-1	-6.0930E-2	3.9763E-3	-1.5825E-4	4.0664E-6
20.5	-1.4876E-1	4.7650E-1	-5.6828E-2	3.5835E-3	-1.3792E-4	3.4304E-6
21.0	-1.4898E-1	4.5930E-1	-5.2740E-2	3.1963E-3	-1.1802E-4	2.8111E-6
21.5	-1.4947E-1	4.4356E-1	-4.8945E-2	2.8349E-3	-9.9395E-5	2.2302E-6
22.0	-1.4915E-1	4.2759E-1	-4.5168E-2	2.4786E-3	-8.1146E-5	1.6638E-6
22.5	-1.4812E-1	4.1307E-1	-4.1789E-2	2.1628E-3	-6.5078E-5	1.1673E-6
23.0	-1.4652E-1	3.9849E-1	-3.8450E-2	1.8536E-3	-4.9433E-5	6.8604E-7
23.5	-1.4427E-1	3.8385E-1	-3.5162E-2	1.5525E-3	-3.4328E-5	2.2407E-7
24.0	-1.4156E-1	3.6922E-1	-3.1929E-2	1.2592E-3	-1.9703E-5	-2.2109E-7
24.5	-1.3862E-1	3.5526E-1	-2.8874E-2	9.8401E-4	-6.0481E-6	-6.3518E-7
25.0	-1.3532E-1	3.4139E-1	-2.5881E-2	7.1663E-4	7.1340E-6	-1.0330E-6

4. Numerical results

The derived expressions for the absorption coefficient k_{abs} can be used to calculate the cloud emittance ϵ [Eq. (1)] as a function of the bulk parameter W (total water content) and as a function of the size distribution parameters α and β , or r_0 and s , or r_{eff} and v_{eff} .

The derived expressions for the absorption coefficient k_{abs} are relatively simple when compared to the Mie scattering calculation and integration over the size distribution. The number of terms N kept in the summations for the absorption efficiency [Eq. (9)] or the absorption coefficients [Eqs. (30) and (38)] is determined by the required accuracy.

Within the atmospheric window from 8 to 13 μm ,

the Q_{abs} behavior as a function of the droplet's radius is similar to that shown in Fig. 2. The dashed lines represent the fourth- and the sixth-order polynomial fits of the type of Eq. (9) to the Mie Q_{abs} curve (solid line). It is apparent that the sixth-order polynomial fit provides an acceptable approximation to the exact Mie calculations at all radii $r < 100 \mu\text{m}$. Unfortunately, at some wavelengths outside the atmospheric window the sixth-order polynomial does not provide an equally accurate approximation to the Mie calculated Q_{abs} curve. The situation depicted in Fig. 3 gives an example of such a case occurring at the wavelength of 17 μm . The tenth-order polynomial is required to approximate the Q_{abs} curve at $\lambda = 17 \mu\text{m}$ with a sufficient accuracy at radii $r < 100 \mu\text{m}$.

For the sake of uniformity we have decided to use the tenth-order polynomial fit at all wavelengths. The coefficients a_n of the polynomial fit for water droplets at a set of wavelengths between 3 and 25 μm are listed in Tables 2a and 2b. Refractive indices of water are taken from Hale and Querry (1973). When the values of refractive indices at the half-micrometer steps were not available, the values used were obtained by linear interpolation between the nearest available wavelengths.

The test of the approximation comes, of course, from the comparison of the approximate results for the absorption coefficient k_{abs} and the exact Mie calculations. We have chosen several typical size distributions

(Shettle 1989) of cumulus, stratus, stratocumulus, altostratus, and nimbostratus clouds, as well as size distributions representing a moderate radiation fog and a heavy advection fog for which the absorption coefficients from exact Mie scattering calculations were already available in the LOWTRAN7 atmospheric transmittance/radiance code (Kneizys et al. 1988). The gamma-size distribution parameters for these models and the corresponding values of v_{eff} and r_{eff} are listed in Table 3.

The values of the absorption coefficient k_{abs} for these cloud models at wavelengths that are integer multiples of 0.5 μm were selected for comparison with the values of the absorption coefficient calculated using the ex-

TABLE 2b. Expansion coefficients, a_6 - a_{10} , from the tenth-order polynomial fit to water drops, with $r \leq 100 \mu\text{m}$.

Wavelength (μm)	a_6	a_7	a_8	a_9	a_{10}
3.0	-2.2389E-07	2.8622E-09	-2.2544E-11	9.9746E-14	-1.8966E-16
3.5	-6.0609E-09	5.9481E-11	-3.6081E-13	1.2218E-15	-1.7486E-18
4.0	1.0261E-08	-1.3766E-10	1.1202E-12	-5.0720E-15	9.8090E-18
4.5	1.9928E-08	-2.6942E-10	2.2012E-12	-9.9883E-15	1.9341E-17
5.0	2.1738E-08	-2.8289E-10	2.2459E-12	-9.9626E-15	1.8936E-17
5.5	1.2276E-08	-1.4685E-10	1.0815E-12	-4.4834E-15	8.0127E-18
6.0	-8.1347E-08	9.6468E-10	-7.1655E-12	3.0252E-14	-5.5365E-17
6.5	2.5868E-08	-3.4911E-10	2.8294E-12	-1.2710E-14	2.4354E-17
7.0	1.7944E-08	-2.2171E-10	1.6744E-12	-7.0907E-15	1.2918E-17
7.5	9.7169E-09	-1.1158E-10	7.8579E-13	-3.1149E-15	5.3321E-18
8.0	5.6288E-09	-6.2224E-11	4.2516E-13	-1.6499E-15	2.7899E-18
8.5	5.3008E-09	-6.3495E-11	4.7454E-13	-2.0219E-15	3.7498E-18
9.0	6.5504E-09	-8.4066E-11	6.6509E-13	-2.9626E-15	5.6808E-18
9.5	7.6356E-09	-1.0032E-10	8.0478E-13	-3.6110E-15	6.9446E-18
10.0	7.6913E-09	-1.0243E-10	8.2657E-13	-3.7160E-15	7.1456E-18
10.5	5.6257E-09	-8.0418E-11	6.7535E-13	-3.1129E-15	6.0877E-18
11.0	-3.4994E-09	2.3784E-11	-7.6205E-14	-1.2891E-17	5.1931E-19
11.5	-2.6303E-08	2.9690E-10	-2.1192E-12	8.6571E-15	-1.5412E-17
12.0	-6.1215E-08	7.2636E-10	-5.3985E-12	2.2803E-14	-4.1747E-17
12.5	-9.8069E-08	1.1853E-09	-8.9365E-12	3.8182E-14	-7.0562E-17
13.0	-1.2376E-07	1.5065E-09	-1.1421E-11	4.9013E-14	-9.0900E-17
13.5	-1.4329E-07	1.7503E-09	-1.3305E-11	5.7215E-14	-1.0629E-16
14.0	-1.5509E-07	1.8960E-09	-1.4422E-11	6.2045E-14	-1.1530E-16
14.5	-1.6058E-07	1.9617E-09	-1.4911E-11	6.4115E-14	-1.1909E-16
15.0	-1.6305E-07	1.9890E-09	-1.5101E-11	6.4862E-14	-1.2037E-16
15.5	-1.6380E-07	1.9945E-09	-1.5119E-11	6.4858E-14	-1.2023E-16
16.0	-1.6162E-07	1.9625E-09	-1.4842E-11	6.3550E-14	-1.1762E-16
16.5	-1.5769E-07	1.9083E-09	-1.4393E-11	6.1484E-14	-1.1357E-16
17.0	-1.5002E-07	1.9067E-09	-1.3573E-11	5.7789E-14	-1.0645E-16
17.5	-1.4125E-07	1.6913E-09	-1.2644E-11	5.3619E-14	-9.8429E-17
18.0	-1.3002E-07	1.5452E-09	-1.1480E-11	4.8421E-14	-8.8483E-17
18.5	-1.1707E-07	1.3778E-09	-1.0152E-11	4.2520E-14	-7.7227E-17
19.0	-1.0248E-07	1.1902E-09	-8.6712E-12	3.5962E-14	-6.4754E-17
19.5	-8.5696E-08	9.7610E-10	-6.9894E-12	2.8545E-14	-5.0697E-17
20.0	-6.8867E-08	7.6375E-10	-5.3363E-12	2.1306E-14	-3.7054E-17
20.5	-5.6286E-08	6.0532E-10	-4.1048E-12	1.5919E-14	-2.6915E-17
21.0	-4.4081E-08	4.5209E-10	-2.9165E-12	1.0732E-14	-1.7164E-17
21.5	-3.2619E-08	3.0803E-10	-1.7986E-12	5.8488E-15	-7.9824E-18
22.0	-2.1481E-08	1.6844E-10	-7.1772E-13	1.1361E-15	8.6640E-19
22.5	-1.1753E-08	4.6831E-11	2.2203E-13	-2.9546E-15	8.5368E-18
23.0	-2.3533E-09	-7.0363E-11	1.1258E-12	-6.8819E-15	1.5891E-17
23.5	6.6294E-09	-1.8198E-10	1.9841E-12	-1.0604E-14	2.2847E-17
24.0	1.5254E-08	-2.8884E-10	2.8041E-12	-1.4152E-14	2.9469E-17
24.5	2.3254E-08	-3.8774E-10	3.5615E-12	-1.7426E-14	3.5570E-17
25.0	3.0913E-08	-4.8214E-10	4.2829E-12	-2.0537E-14	4.1360E-17

TABLE 3. Parameters for the model cloud and fog size distributions.

Cloud type	α	β	A	W ($g\ m^{-3}$)	r_{eff} (μm)	v_{eff}
Cumulus	3	0.5	2.604	1.00	12.0	0.167
Altostratus	5	1.111	6.268	0.41	7.2	0.125
Stratus	2	0.6	27.0	0.29	8.33	0.200
Stratus/stratocumulus	2	0.75	52.734	0.15	6.67	0.200
Nimbostratus	2	0.425	7.676	0.65	11.76	0.200
Advection fog	3	0.3	0.027	0.37	20.0	0.167
Radiation fog	6	3.0	607.5	0.015	3.0	0.111

pansion, Eq. (29) or (10), based on the tenth-order polynomial fit (9) to Q_{abs} . Restricting the comparisons to only these wavelengths avoided introducing uncertainties due to possible inaccuracies in interpolating to other wavelengths, either the values for LOWTRAN or for the expansion. The appropriate values for the a_n from Table 2 were used in (29).

Except for the radiation fog model, the error is within 1.1% at most wavelengths. For the wavelengths of 3 μm and $20\ \mu m < \lambda < 25\ \mu m$, the maximum error reaches a value of 2.7%. At the same time, the computer time required to perform the calculation of k_{abs} is reduced by a factor of 10^4 to 10^5 compared to the Mie calculations with integration over the size distribution.

The case of radiation-fog size distribution shows an error twice as large as any other considered case (up to 2.6% for $3.5 < \lambda < 20\ \mu m$ and 6.5% at $\lambda = 25\ \mu m$). This is caused by the fact that this narrow ($v_{eff} = 0.11$) size distribution is dominated by small droplets ($r_{mode} = 2\ \mu m$) and that the polynomial fit to the Q_{abs} , as given by expression (9), is not constrained to go to zero at $r = 0$. The latter could be accomplished by presetting $a_0 = 0$, which on the other hand would de-

TABLE 4. Expansion coefficients for three-term quadratic fit to water absorption efficiency [Eq. (9)] for $r \leq 20\ \mu m$.

Wavelength (μm)	a_0	a_1	a_2
3.0	1.0752E+0	1.8942E-2	-1.3104E-3
3.5	1.9418E-2	7.1036E-2	-1.8280E-3
4.0	-1.0043E-2	3.6936E-2	-7.4394E-4
4.5	-8.7037E-3	8.1747E-2	-2.1420E-3
5.0	-1.6449E-2	7.0899E-2	-1.6838E-3
5.5	-1.6316E-2	5.8596E-2	-1.1650E-3
6.0	3.0081E-1	1.5072E-1	-5.8461E-3
6.5	1.6005E-2	1.3270E-1	-4.1574E-3
7.0	-9.6504E-3	1.0972E-1	-3.0003E-3
7.5	-1.2594E-2	1.0362E-1	-2.6884E-3
8.0	-1.3211E-2	1.0026E-1	-2.5135E-3
8.5	-1.2544E-2	9.8262E-2	-2.4076E-3
9.0	-1.0594E-2	9.7506E-2	-2.3650E-3
9.5	-7.0447E-3	9.8052E-2	-2.3886E-3
10.0	-4.0922E-4	9.9981E-2	-2.4881E-3
10.5	1.9190E-2	1.0929E-1	-2.9496E-3
11.0	6.6452E-2	1.2421E-1	-3.7771E-3
11.5	1.4524E-1	1.3467E-1	-4.5311E-3
12.0	2.4481E-1	1.3844E-1	-5.0234E-3
12.5	3.4206E-1	1.3956E-1	-5.3509E-3
13.0	4.0654E-1	1.4020E-1	-5.5531E-3
13.5	4.5224E-1	1.4173E-1	-5.7438E-3
14.0	4.7611E-1	1.4456E-1	-5.9388E-3
14.5	4.8337E-1	1.4833E-1	-6.1360E-3
15.0	4.8317E-1	1.5243E-1	-6.3304E-3
15.5	4.7913E-1	1.5659E-1	-6.5183E-3
16.0	4.6823E-1	1.6140E-1	-6.7193E-3
16.5	4.5414E-1	1.6623E-1	-6.9127E-3
17.0	4.3258E-1	1.7157E-1	-7.1088E-3
17.5	4.0957E-1	1.7693E-1	-7.3017E-3
18.0	3.8280E-1	1.8221E-1	-7.4778E-3
18.5	3.5380E-1	1.8733E-1	-7.6374E-3
19.0	3.2274E-1	1.9222E-1	-7.7772E-3
19.5	2.8857E-1	1.9679E-1	-7.8872E-3
20.0	2.5584E-1	1.9978E-1	-7.9170E-3
20.5	2.3169E-1	2.0194E-1	-7.9331E-3
21.0	2.0840E-1	2.0379E-1	-7.9353E-3
21.5	1.8657E-1	2.0571E-1	-7.9455E-3
22.0	1.6545E-1	2.0738E-1	-7.9454E-3
22.5	1.4713E-1	2.0871E-1	-7.9368E-3
23.0	1.2945E-1	2.0983E-1	-7.9198E-3
23.5	1.1257E-1	2.1069E-1	-7.8911E-3
24.0	9.6363E-2	2.1134E-1	-7.8537E-3
24.5	8.1372E-2	2.1182E-1	-7.8117E-3
25.0	6.6971E-2	2.1215E-1	-7.7632E-3

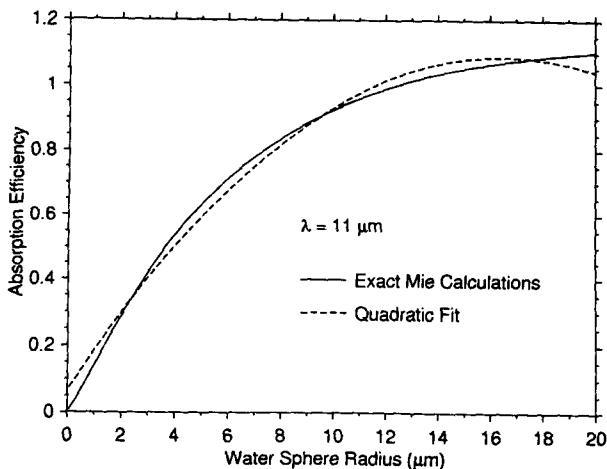


FIG. 4. An example of a quadratic fit for the case of small water droplets with radii $r < 20\ \mu m$.

TABLE 5a. Expansion coefficients, a_0 - a_5 , from the tenth-order polynomial fit to ice spheres, with $r \leq 100 \mu\text{m}$.

Wavelength (μm)	a_0	a_1	a_2	a_3	a_4	a_5
3.0	8.9107E-1	1.6530E-1	-3.7508E-2	3.6395E-3	-1.9366E-4	6.2286E-6
3.5	-5.7954E-2	2.0296E-1	-2.2180E-2	1.5170E-3	-6.6013E-5	1.8606E-6
4.0	-2.7474E-2	8.3809E-2	-3.4359E-3	-5.2990E-6	7.8409E-6	-3.8786E-7
4.5	-5.6616E-2	2.0473E-1	-1.5734E-2	5.9829E-4	-9.5388E-6	-8.4868E-8
5.0	-1.2676E-2	6.0765E-2	1.6553E-3	-4.5993E-4	2.9855E-5	-1.0334E-6
5.5	-1.7730E-2	9.6300E-2	-1.7298E-4	-4.3812E-4	3.0518E-5	-1.0537E-6
6.0	-5.5578E-2	2.8438E-1	-2.7057E-2	1.3910E-3	-4.3868E-5	8.9189E-7
6.5	-5.4572E-2	2.3325E-1	-1.7265E-2	5.7691E-4	-5.6062E-6	-2.2378E-7
7.0	-5.0451E-2	2.1098E-1	-1.3570E-2	3.1979E-4	4.3274E-6	-4.5926E-7
7.5	-4.3692E-2	1.7941E-1	-9.0475E-3	4.6696E-5	1.3304E-5	-6.3184E-7
8.0	-3.5263E-2	1.4141E-1	-4.5979E-3	-1.6103E-4	1.7624E-5	-6.4189E-7
8.5	-2.8235E-2	1.1215E-1	-2.7109E-3	-1.3103E-4	1.0889E-5	-3.5197E-7
9.0	-2.7612E-2	1.1313E-1	-3.0835E-3	-9.5918E-5	9.7101E-6	-3.4219E-7
9.5	-2.5015E-2	1.1047E-1	-3.0437E-3	-9.0775E-5	9.8476E-6	-3.6493E-7
10.0	-2.0375E-2	1.1000E-1	-3.5467E-3	-4.0922E-5	7.7393E-6	-3.1188E-7
10.5	-2.1607E-2	2.0223E-1	-1.6960E-2	8.6724E-4	-2.9286E-5	6.6965E-7
11.0	2.9596E-2	3.9822E-1	-5.7009E-2	4.3543E-3	-1.9985E-4	5.8168E-6
11.5	8.2413E-2	5.0745E-1	-8.1752E-2	6.6671E-3	-3.1876E-4	9.5357E-6
12.0	7.5458E-2	5.7059E-1	-9.4667E-2	7.8252E-3	-3.7690E-4	1.1326E-5
12.5	2.2052E-2	6.1442E-1	-1.0147E-1	8.3351E-3	-3.9923E-4	1.1942E-5
13.0	-5.9200E-2	6.3032E-1	-1.0043E-1	8.0336E-3	-3.7724E-4	1.1115E-5
13.5	-1.3165E-1	6.1274E-1	-9.1711E-2	6.9954E-3	-3.1670E-4	9.0693E-6
14.0	-1.7738E-1	5.6126E-1	-7.6248E-2	5.3609E-3	-2.2675E-4	6.1354E-6
14.5	-1.8483E-1	4.6432E-1	-5.2605E-2	3.0688E-3	-1.0703E-4	2.3682E-6
15.0	-1.5743E-1	3.5311E-1	-2.9141E-2	9.8515E-4	-4.8332E-6	-6.9700E-7
15.5	-1.2435E-1	2.6912E-1	-1.3768E-2	-2.3246E-4	4.9399E-5	-2.1949E-6
16.0	-1.0097E-1	2.1765E-1	-5.5976E-3	-7.9049E-4	7.0690E-5	-2.6945E-6
16.5	-8.7180E-2	1.8861E-1	-1.5200E-3	-1.0262E-3	7.7784E-5	-2.8080E-6
17.0	-7.4294E-2	1.5896E-1	2.4995E-3	-1.2532E-3	8.4492E-5	-2.9130E-6
17.5	-5.7231E-2	1.2262E-1	6.2487E-3	-1.3727E-3	8.3415E-5	-2.7352E-6
18.0	-4.2640E-2	9.2520E-2	8.0308E-3	-1.3026E-3	7.3106E-5	-2.2921E-6
18.5	-3.4318E-2	7.5940E-2	8.2279E-3	-1.1722E-3	6.2842E-5	-1.9207E-6
19.0	-3.0230E-2	6.8795E-2	8.1714E-3	-1.1059E-3	5.8413E-5	-1.7791E-6
19.5	-2.8816E-2	6.6579E-2	8.4796E-3	-1.1282E-3	5.9604E-5	-1.8228E-6
20.0	-2.3196E-2	5.3772E-2	8.5749E-3	-1.0412E-3	5.3268E-5	-1.6052E-6
20.5	-1.5725E-2	3.7466E-2	7.6962E-3	-8.3747E-4	4.1373E-5	-1.2392E-6
21.0	-1.0164E-2	2.6553E-2	6.8723E-3	-7.0518E-4	3.4928E-5	-1.0705E-6
21.5	-6.2522E-3	1.9677E-2	6.4045E-3	-6.4095E-4	3.2236E-5	-1.0091E-6
22.0	-2.9938E-3	1.3785E-2	5.8087E-3	-5.6911E-4	2.8945E-5	-9.1667E-7
22.5	-1.0285E-3	1.0359E-2	5.2738E-3	-5.0751E-4	2.5793E-5	-8.1411E-7
23.0	-1.3748E-4	9.2250E-3	4.9834E-3	-4.7251E-4	2.3769E-5	-7.4112E-7
23.5	3.6987E-4	8.8727E-3	4.8006E-3	-4.4914E-4	2.2313E-5	-6.8647E-7
24.0	7.9012E-4	8.7828E-3	4.6980E-3	-4.3504E-4	2.1388E-5	-6.5096E-7
24.5	1.2440E-3	8.6896E-3	4.6314E-3	-4.2580E-4	2.0793E-5	-6.2877E-7
25.0	1.7141E-3	8.7478E-3	4.6382E-3	-4.2512E-4	2.0693E-5	-6.2406E-7

crease the accuracy of the fit at larger values of the droplet radius.

5. Small- and large-particle approximations

For the purposes of theoretical investigation, as well as for simplicity of the modeling, it is sometimes useful to obtain a simple analytical form (valid within a restricted region of r) for the k_{abs} , even if the high degree of accuracy has to be compromised.

If the radii of most of the particles present in the cloud are below $20 \mu\text{m}$, the first few terms of expression (20) will be sufficient to determine the absorption coef-

ficient. Keeping only terms up to the second power in radius r , we obtain

$$k_{\text{abs}} = \frac{3W}{4\rho} \left[\frac{a_0}{r_{\text{eff}}} + a_1 + a_2 r_{\text{eff}} (1 + v_{\text{eff}}) \right]. \quad (44)$$

The a_0 , a_1 , and a_2 coefficients in Eq. (44) have to be determined by the best quadratic fit [Eq. (9) with $N = 2$] to the Mie absorption efficiency Q_{abs} within the radii range $0 < r < 20 \mu\text{m}$. Figure 4 shows an example of a quadratic fit to the Mie absorption efficiency for water droplets with $0 < r < 20 \mu\text{m}$. The coefficients at the half micron steps for the wavelengths from 3 to 25

TABLE 5b. Expansion coefficients, a_6 – a_{10} , from the tenth-order polynomial fit to ice spheres, with $r \leq 100 \mu\text{m}$.

Wavelength (μm)	a_6	a_7	a_8	a_9	a_{10}
3.0	-1.2627E-07	1.6239E-09	-1.2850E-11	5.7068E-14	-1.0884E-16
3.5	-3.4310E-08	4.1052E-10	-3.0679E-12	1.3003E-14	-2.3852E-17
4.0	9.6259E-09	-1.3951E-10	1.1947E-12	-5.6112E-15	1.1157E-17
4.5	6.6071E-09	-1.2691E-10	1.2391E-12	-6.2740E-15	1.3091E-17
5.0	2.1626E-08	-2.8198E-10	2.2424E-12	-9.9617E-15	1.8959E-17
5.5	2.1671E-08	-2.7685E-10	2.1579E-12	-9.4087E-15	1.7603E-17
6.0	-1.1846E-08	1.0116E-10	-5.2673E-13	1.4794E-15	-1.6184E-18
6.5	9.0737E-09	-1.5143E-10	1.3711E-12	-6.5925E-15	1.3225E-17
7.0	1.2630E-08	-1.8564E-10	1.5729E-12	-7.2516E-15	1.4125E-17
7.5	1.4536E-08	-1.9578E-10	1.5707E-12	-6.9686E-15	1.3187E-17
8.0	1.3104E-08	-1.6359E-10	1.2422E-12	-5.2813E-15	9.6579E-18
8.5	6.6279E-09	-7.8216E-11	5.7184E-13	-2.3747E-15	4.2885E-18
9.0	6.9789E-09	-8.8893E-11	6.9707E-13	-3.0792E-15	5.8621E-18
9.5	7.7636E-09	-1.0215E-10	8.1995E-13	-3.6800E-15	7.0785E-18
10.0	6.8737E-09	-9.1971E-11	7.4375E-13	-3.3464E-15	6.4364E-18
10.5	-1.0396E-08	1.0775E-10	-7.1287E-13	2.7199E-15	-4.5510E-18
11.0	-1.0977E-07	1.3379E-09	-1.0154E-11	4.3620E-14	-8.0970E-17
11.5	-1.8350E-07	2.2690E-09	-1.7414E-11	7.5464E-14	-1.4108E-16
12.0	-2.1858E-07	2.7083E-09	-2.0817E-11	9.0312E-14	-1.6898E-16
12.5	-2.2962E-07	2.8364E-09	-2.1746E-11	9.4145E-14	-1.7584E-16
13.0	-2.1122E-07	2.5850E-09	-1.9669E-11	8.4622E-14	-1.5723E-16
13.5	-1.6850E-07	2.0249E-09	-1.5179E-11	6.4496E-14	-1.1858E-16
14.0	-1.0869E-07	1.2546E-09	-9.0860E-12	3.7477E-14	-6.7148E-17
14.5	-3.3904E-08	3.1078E-10	-1.7413E-12	5.3340E-15	-6.6234E-18
15.0	2.4693E-08	-4.0649E-10	3.7025E-12	-1.7997E-14	3.6537E-17
15.5	5.1361E-08	-7.1333E-10	5.9083E-12	-2.7009E-14	5.2514E-17
16.0	5.8834E-08	-7.8453E-10	6.3238E-12	-2.8348E-14	5.4310E-17
16.5	5.9562E-08	-7.7974E-10	6.2052E-12	-2.7556E-14	5.2415E-17
17.0	6.0192E-08	-7.7450E-10	6.0881E-12	-2.6789E-14	5.0596E-17
17.5	5.4775E-08	-6.8966E-10	5.3361E-12	-2.3202E-14	4.3423E-17
18.0	4.4567E-08	-5.4979E-10	4.1931E-12	-1.8047E-14	3.3529E-17
18.5	3.6803E-08	-4.5050E-10	3.4242E-12	-1.4729E-14	2.7395E-17
19.0	3.4171E-08	-4.2053E-10	3.2177E-12	-1.3936E-14	2.6094E-17
19.5	3.5192E-08	-4.3533E-10	3.3462E-12	-1.4549E-14	2.7328E-17
20.0	3.0821E-08	-3.8110E-10	2.9362E-12	-1.2813E-14	2.4165E-17
20.5	2.3997E-08	-3.0115E-10	2.3585E-12	-1.0454E-14	1.9992E-17
21.0	2.1297E-08	-2.7367E-10	2.1831E-12	-9.8071E-15	1.8932E-17
21.5	2.0402E-08	-2.6464E-10	2.1196E-12	-9.5254E-15	1.8355E-17
22.0	1.8624E-08	-2.4133E-10	1.9238E-12	-8.5878E-15	1.6425E-17
22.5	1.6407E-08	-2.1031E-10	1.6566E-12	-7.3089E-15	1.3826E-17
23.0	1.4734E-08	-1.8633E-10	1.4494E-12	-6.3236E-15	1.1845E-17
23.5	1.3468E-08	-1.6824E-10	1.2947E-12	-5.5961E-15	1.0400E-17
24.0	1.2644E-08	-1.5659E-10	1.1966E-12	-5.1437E-15	9.5178E-18
24.5	1.2148E-08	-1.4989E-10	1.1430E-12	-4.9095E-15	9.0880E-18
25.0	1.2041E-08	-1.4862E-10	1.1354E-12	-4.8916E-15	9.0898E-18

μm are given in Table 4. From the parameters for the droplet size distributions, given in Table 3, it is apparent that the small droplet approximation [Eq. (44)] cannot be applied to the advection fog size distribution, which has $r_{\text{eff}} = 20 \mu\text{m}$ and a considerable contribution from droplets with radii $r > 20 \mu\text{m}$, outside the range for which the Q_{abs} fit was made. For the other model size distributions the error is within 3.5% for wavelengths within the atmospheric window. At other wavelengths the error is within 7%, with the exception of radiation fog where the maximum error of 13% occurs at $\lambda = 3 \mu\text{m}$.

If the a_0 and a_2 terms in Eq. (44) for the absorption coefficient are neglected, we recover the simple approximation (5) in the form of liquid water content W . In the case of all droplets being very small (let us say with radii $r < 7 \mu\text{m}$) this approximation leads to accurate results.

It is interesting to note that an approximation in the form of Eq. (44), for the absorption coefficient, can also be derived for large spherical particles if all the radii of the size distribution are larger than about $15 \mu\text{m}$. In this case the quadratic fit to the Mie absorption efficiency between $15 \mu\text{m} < r < 100 \mu\text{m}$ is sufficiently

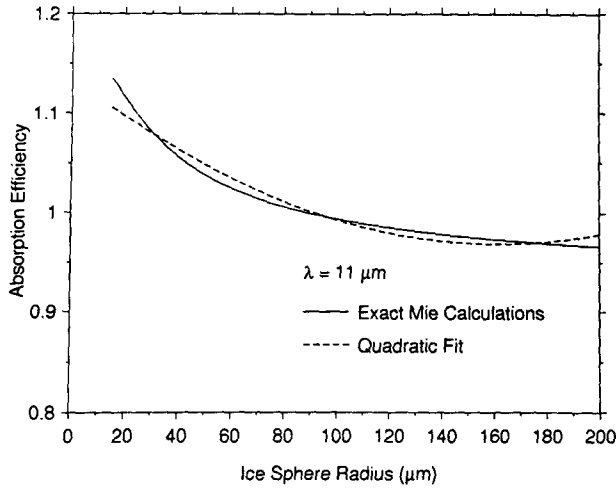


FIG. 5. A quadratic fit to the Mie Q_{abs} curve for the case of equivalent ice spheres with radii $15 \mu\text{m} < r < 200 \mu\text{m}$.

accurate and the a_0 , a_1 , and a_2 coefficients have to be determined by such a fit.

6. Infrared emittance of cirrus clouds

Although the prime goal of this work is to develop a suitable parameterization for the IR emittance of water clouds, the formalism of the preceding sections can be extended to include ice clouds if the ice particles are spherical or if they are modeled by equivalent spheres (Stephens et al. 1990; Ackerman et al. 1990; Smith et al. 1990; Spinhirne and Hart 1990). The formalism described in sections 3 and 5 can be used to obtain the absorption coefficient for considered size distributions of ice spheres. However, the coefficients a_n appearing in expressions (10), (14), (15), and (20) are now determined by the appropriate polynomial fit, [Eq. (9)], to the Mie absorption efficiency for ice spheres. The coefficients for the case of spherical ice particles with radii smaller than 100 microns are listed in Table 5. Refractive indices of ice are taken from Warren's (1984) compilation. Similarly, the coefficients of the small or large particle approximations [Eq. (44)] are now determined by a quadratic polynomial fit to the Mie absorption efficiency curve in the limited region of ice sphere radii. Figure 5 shows an example of a quadratic fit in the large particle approximation. The appropriate expansion coefficients for large cirrus spheres with radii in the region between 15 and 200 μm are given in Table 6.

This approach can also be applied to size distributions of nonspherical ice crystals if suitable results for the absorption efficiency as a function of particle size (Mugnai and Wiscombe 1986; Takano and Liou 1989; Chýlek and Klett 1991) are available.

7. Discussion

It seems that the most important result of the reported research is an approximate formula for the absorption coefficient k_{abs} given by Eq. (44). This expression combines acceptable accuracy and a simple analytical form displaying explicit dependence on the cloud water content W and the size distribution parameters r_{eff} and v_{eff} . Furthermore, it is sufficiently accurate for use in numerical calculations and simple enough to be used in theoretical investigations. Equation (44) for

TABLE 6. Expansion coefficients for three-term quadratic fit to absorption efficiency [Eq. (9)], for ice spheres with $15 \leq r < 200 \mu\text{m}$.

Wavelength (μm)	a_0	a_1	a_2
3.0	9.5794E-01	-9.2305E-04	3.0468E-06
3.5	9.4296E-01	2.6706E-04	-1.8421E-06
4.0	7.1377E-01	4.1147E-03	-1.5766E-05
4.5	1.0458E+00	-9.5638E-04	2.5674E-06
5.0	7.3208E-01	4.0563E-03	-1.5683E-05
5.5	9.5774E-01	7.9723E-04	-4.2035E-06
6.0	1.1456E+00	-2.3116E-03	7.4975E-06
6.5	1.1427E+00	-2.2295E-03	7.0843E-06
7.0	1.1491E+00	-2.2477E-03	7.0580E-06
7.5	1.1460E+00	-2.0909E-03	6.3558E-06
8.0	1.1208E+00	-1.5564E-03	4.2178E-06
8.5	1.0764E+00	-6.4835E-04	6.7678E-07
9.0	1.0904E+00	-7.2532E-04	8.4518E-07
9.5	1.0913E+00	-5.6236E-04	1.0025E-07
10.0	1.0777E+00	-7.9458E-05	-1.8668E-06
10.5	1.1252E+00	-1.0303E-03	2.1463E-06
11.0	1.1359E+00	-2.0739E-03	6.4355E-06
11.5	1.1601E+00	-2.7683E-03	8.8891E-06
12.0	1.1803E+00	-3.1864E-03	1.0316E-05
12.5	1.1991E+00	-3.4947E-03	1.1353E-05
13.0	1.2187E+00	-3.7425E-03	1.2182E-05
13.5	1.2381E+00	-3.9599E-03	1.2912E-05
14.0	1.2572E+00	-4.1655E-03	1.3606E-05
14.5	1.2780E+00	-4.3677E-03	1.4284E-05
15.0	1.2961E+00	-4.5100E-03	1.4728E-05
15.5	1.3069E+00	-4.5381E-03	1.4732E-05
16.0	1.3121E+00	-4.4952E-03	1.4470E-05
16.5	1.3159E+00	-4.4543E-03	1.4227E-05
17.0	1.3130E+00	-4.3234E-03	1.3642E-05
17.5	1.2944E+00	-3.8994E-03	1.1928E-05
18.0	1.2569E+00	-3.1544E-03	9.0080E-06
18.5	1.2214E+00	-2.4586E-03	6.3079E-06
19.0	1.2063E+00	-2.1121E-03	4.9325E-06
19.5	1.2117E+00	-2.1365E-03	4.9546E-06
20.0	1.1589E+00	-1.2267E-03	1.5315E-06
20.5	1.0303E+00	8.4171E-04	-5.9814E-06
21.0	8.9607E-01	2.8562E-03	-1.2973E-05
21.5	7.9121E-01	4.3166E-03	-1.7775E-05
22.0	6.7011E-01	5.8045E-03	-2.2261E-05
22.5	5.7890E-01	6.7967E-03	-2.4954E-05
23.0	5.4330E-01	7.2149E-03	-2.6136E-05
23.5	5.2952E-01	7.4439E-03	-2.6910E-05
24.0	5.2612E-01	7.5908E-03	-2.7529E-05
24.5	5.2431E-01	7.7275E-03	-2.8136E-05
25.0	5.3065E-01	7.8034E-03	-2.8639E-05

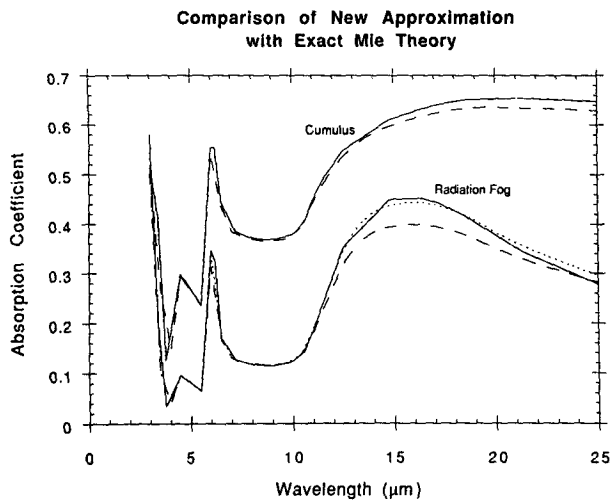


FIG. 6. Comparison of exact Mie calculations (solid line) with the tenth-order polynomial approximation (dotted line) and with the second-order polynomial approximation (dashed line). The cumulus cloud has the minimum error (the dotted line cannot be distinguished from the exact Mie calculation), and the radiation fog has the maximum error from the set of considered size distributions.

the k_{abs} coefficient is also independent of the specific form of the size distribution used. The accuracy of Eq. (44) is within 7% in the small particle approximation for all considered cloud types at the wavelengths between 3 and 25 μm . The only information required is the cloud water content, the effective radius, and the effective variance (W , r_{eff} , and v_{eff}), or the second, third, and fourth moments of the size distribution.

This result supports the conclusions of Hansen and Travis (1974) that the Mie scattering properties of different size distributions were nearly the same if the size distributions had the same values of effective radius and effective variance, with the effective radius being the most critical parameter. To examine this further, the cloud model size distributions were replaced by equivalent monodisperse distributions with r_{eff} as the radius and the effective variance $v_{\text{eff}} = 0$. This is equivalent to using Eq. (15) for the absorption coefficient with all the $D_k = 1$. Using the second-order approximation for the absorption efficiency [Eq. (44)] gave rms errors compared with the exact Mie results of 10% or better. This was true even for the advection fog model, where the effective radius was 20 μm . Using the correct value of the effective variance in a small particle approximation given by Eq. (44) would give a maximum error of nearly 60%. This is because any polynomial expansion, such as Eq. (9), for absorption efficiency will often have an extreme divergence from the correct values outside the range of the fit, which here was restricted to $r \leq 20 \mu\text{m}$.

If the more accurate results are desirable or if the size distributions of water drops with $r > 20 \mu\text{m}$ are

considered, the higher-order expansion, Eq. (10) or its equivalents in the form of Eqs. (14), (15), (20), (29), (30), or (38), can be used. These expressions are suitable for fast numerical calculations and are accurate within 3% for considered cloud types. However, a simple analytical dependence of k_{abs} on the size distribution parameters is lost. Alternatively, the equivalent of second-order expansion, Eq. (44), can be fit for large water droplets. Comparison of the absorption coefficient, calculated using the exact Mie calculation (2), the tenth-order polynomial fit (10), and the quadratic fit (44) is shown in Fig. 6 as a function of wavelength for the cases of the cumulus cloud and the radiation fog.

Acknowledgments. The reported research was supported in part by the Atmospheric Environment Service and the Natural Sciences and Engineering Research Council of Canada and by the USN Office of Naval Technology. This work was completed while the first author was at the Naval Research Laboratory, under the U.S. Navy–ASEE Summer Faculty Research Program.

REFERENCES

- Abramowitz, M., and I. A. Stegun, 1964: *Handbook of Mathematical Functions*. U.S. Govt. Printing Office, 1046 pp.
- Ackerman, S. A., W. L. Smith, J. D. Spinhirne, and H. E. Revercomb, 1990: The 27–28 October 1986 FIRE IFO cirrus case study: Spectral properties of cirrus clouds in the 8–12 μm window. *Mon. Wea. Rev.*, **118**, 2377–2388.
- Aitchison, J., and J. A. C. Brown, 1957: *The Lognormal Distribution, with Special Reference to Its Uses in Economics*. Cambridge University Press, 7–13.
- Allen, T., 1968: *Particle Size Measurement*. Chapman and Hall, 95–97.
- d’Almeida, G. A., P. Koepke, and E. P. Shettle, 1991: *Atmospheric Aerosols, Global Climatology and Radiative Characteristics*. A. Deepak, 561 pp.
- Carrier, L. W., G. A. Cate, and K. J. von Essen, 1967: The backscattering and extinction of visible and IR radiation by selected major cloud models. *Appl. Opt.*, **12**, 555–563.
- Charlock, T. P., 1982: Cloud optics as possible stabilizing factor in climate. *J. Atmos. Sci.*, **38**, 661–663.
- Chýlek, P., 1978: Extinction and liquid water content of fogs and clouds. *J. Atmos. Sci.*, **35**, 296–300.
- , and V. Ramaswamy, 1982: Simple approximation for infrared emissivity of water clouds. *J. Atmos. Sci.*, **39**, 171–177.
- , and J. D. Klett, 1991: Extinction cross sections of nonspherical particles in the anomalous diffraction approximation. *J. Opt. Soc. Amer.*, **A8**, 274–281.
- Clark, W. E., and K. T. Whitby, 1967: Concentration and size distribution measurements of atmospheric aerosol and text of the theory of self-preserving distributions. *J. Atmos. Sci.*, **24**, 677–687.
- Cox, S. K., 1976: Observation of cloud infrared effective emissivity. *J. Atmos. Sci.*, **33**, 287–289.
- Deirmendjian, D., 1969: *Electromagnetic Scattering on Spherical Polydispersions*. Elsevier, 290 pp.
- Hale, G. M., and M. R. Querry, 1973: Optical constants of water in the 200 nm to 200 μm wavelength region. *Appl. Opt.*, **12**, 555–563.
- Hansen, J. E., and L. D. Travis, 1974: Light scattering in planetary atmospheres. *Space Sci. Rev.*, **16**, 527–610.
- Heymsfield, A. J., 1986: Ice particles observed in a cirriform cloud

- at -83°C and implications for polar stratospheric clouds. *J. Atmos. Sci.*, **43**, 851–855.
- , K. M. Miller, and J. D. Spinhirne, 1990: The 27–28 October 1986 FIRE IFO cirrus case study: Cloud microstructure. *Mon. Wea. Rev.*, **118**, 2313–2328.
- Hunt, G. E., 1973: Radiative properties of terrestrial clouds at visible and infrared thermal window wavelengths. *Quart. J. Roy. Meteor. Soc.*, **99**, 346–369.
- Kneizys, F. X., E. P. Shettle, L. W. Abreu, G. P. Anderson, J. H. Chetwynd, W. O. Gallery, J. E. A. Selby, and S. A. Clough, 1988: Users Guide to LOWTRAN 7, AFGL-TR-88-0177. [Available from NTIS AD A206773.]
- Liou, K. N., 1980: *An Introduction to Atmospheric Radiation*. Academic Press, 392 pp.
- Mugnai, A., and W. J. Wiscombe, 1986: Scattering from nonspherical Chebyshev particles. I: Cross sections, single scattering albedo, asymmetry factor, and backscattered fraction. *Appl. Opt.*, **25**, 1235–1244.
- Ohring, G., and P. Clapp, 1980: The effect of changes in cloud amount on the net radiation at the top of the atmosphere. *J. Atmos. Sci.*, **37**, 447–454.
- Paltridge, G. W., 1974: Infrared emissivity, shortwave albedo and the microphysics of stratiform water clouds. *J. Geophys. Res.*, **79**, 4053–4058.
- , 1980: Cloud-radiation feedback to climate. *Quart. J. Roy. Meteor. Soc.*, **106**, 895–899.
- , and C. M. R. Platt, 1976: *Radiative Processes in Meteorology and Climatology*. Elsevier, 318 pp.
- Pinnick, R. G., S. G. Jennings, P. Chýlek, and H. J. Auvermann, 1979: Verification of a linear relation between IR extinction, absorption and liquid water content of fogs. *J. Atmos. Sci.*, **36**, 1577–1586.
- Pinnick, R. G., S. G. Jennings, and P. Chýlek, 1980: Relationship between extinction, absorption, backscattering and mass content of sulfuric acid aerosols. *J. Geophys. Res.*, **85**, 4059–4066.
- Platt, C. M. R., 1975: Infrared emissivity of cirrus—simultaneous satellite, lidar and radiometric observations. *Quart. J. Roy. Meteor. Soc.*, **101**, 119–126.
- , 1976: Infrared absorption and liquid water content in stratocumulus clouds. *Quart. J. Roy. Meteor. Soc.*, **102**, 553–561.
- , 1981: The effect of cirrus of varying optical depth on the extraterrestrial net radiative flux. *Quart. J. Roy. Meteor. Soc.*, **107**, 671–678.
- , and G. L. Stephens, 1980: The interpretation of remotely sensed high cloud emittances. *J. Atmos. Sci.*, **37**, 2314–2322.
- , and Harshvardhan, 1988: Temperature dependence of cirrus extinction: Implications for climate feedback. *J. Geophys. Res.*, **93**, 11 051–11 058.
- , J. S. Scott, and A. C. Dilley, 1987: Remote sounding of high clouds. Part VI: Optical properties of midlatitude and tropical cirrus. *J. Atmos. Sci.*, **44**, 729–747.
- Ramanathan, V., E. J. Pitcher, R. C. Malone, and M. L. Blackman, 1983: The response of a spectral general circulation model to refinements in radiative processes. *J. Atmos. Sci.*, **40**, 605–630.
- Rossow, W. B., and R. A. Schiffer, 1991: ISCCP cloud data products. *Bull. Amer. Meteor. Soc.*, **72**, 2–20.
- Schneider, S., 1972: Cloudiness as a global climate feedback mechanism: The effects on the radiation balance and surface temperature of variations in cloudiness. *J. Atmos. Sci.*, **29**, 1413–1422.
- Shettle, E. P., 1989: Models of aerosols, clouds, and precipitation for atmospheric propagation studies. *AGARD Conf. Proc. CP No. 454, Atmospheric Propagation in the UV, Visible, IR, and mm-Wave Region and Related Systems Aspects*, 15.1–15.3. [Available from NTIS N90-21919.]
- Smith, W. L., P. F. Hein, and S. K. Cox, 1990: The 27–28 October 1986 FIRE IFO study: In situ observations of radiation and dynamic properties of a cirrus cloud layer. *Mon. Wea. Rev.*, **118**, 2389–2401.
- Somerville, R. C. J., and L. A. Remer, 1984: Cloud optical thickness feedbacks in the CO_2 climate problem. *J. Geophys. Res.*, **89**, 9668–9672.
- Spinhirne, J. D., and W. D. Hart, 1990: Cirrus structure and radiative parameters from airborne lidar spectral radiometer observations: The 28 October 1986 FIRE study. *Mon. Wea. Rev.*, **118**, 2329–2343.
- Starr, D. O., 1987: A cirrus cloud experiment: Intensive field observations planned for FIRE. *Bull. Amer. Meteor. Soc.*, **68**, 119–124.
- Stephens, G. L., 1978: Radiation profiles in extended water clouds. II: Parametrization schemes. *J. Atmos. Sci.*, **35**, 2123–2132.
- , 1980: Radiative properties of cirrus clouds in the infrared region. *J. Atmos. Sci.*, **37**, 435–446.
- , 1984: The parametrization of radiation for numerical weather prediction and climate models. *Mon. Wea. Rev.*, **112**, 826–867.
- , and S. C. Tsay, 1990: On cloud absorption anomaly. *Quart. J. Roy. Meteor. Soc.*, **116**, 671–704.
- , —, P. W. Stackhouse, and P. J. Flatau, 1990: The relevance of the microphysical and radiative properties of cirrus clouds to climate and climatic feedback. *J. Atmos. Sci.*, **47**, 1742–1753.
- Takano, Y., and K. N. Liou, 1989: Solar radiative transfer in cirrus clouds. Part I: Single-scattering and optical properties of hexagonal ice crystals. *J. Atmos. Sci.*, **46**, 3–36.
- van de Hulst, H. C., 1957: *Light Scattering by Small Particles*. Dover, 470 pp.
- Warren, S. G., 1984: Optical constants of ice from the ultraviolet to the microwave. *Appl. Opt.*, **23**, 1206–1225.